Gazi University Journal of Science
GU J Sci
28(2):301-310 (2015)

An Analytical Solution of Bimetal Rod Extrusion Process Through Conical Dies

H. HAGHIGHAT[1,♠], H. ASKAR[1]

[1]*Engineering Department, Razi University, Kermanshah, Iran*

Received: 22/10/2014 Accepted:04/03/2015

ABSTRACT

In the present article, the radial and peripheral velocity components are determined for mono-metal rod extrusion through conical dies and then they are extended to extrusion process of initially bonded bimetal rods. By optimizing the total power with respect to the shape of the inlet shear boundary, the amount of extrusion force is obtained. The obtained solutions are tested with other ones found in the literature about this theme and with the results produced by the finite element method. It is found that all of the predicted results are in good agreement with the values computed by the finite element method and experimental results.

Keywords: *Rod Extrusion, Velocity Field, Upper Bound Method*

1. INTRODUCION

The first step in modeling of a metal forming process by the upper bound method is to choose a velocity field for the material undergoing plastic deformation. The accuracy of predictions, load and metal flow, strongly depends on the kinematically admissible velocity field chosen. It is always desirable to utilize a velocity field, which is as close to reality as possible. Even though the velocity field may not match the flow behavior of the workpiece exactly, if it is chosen with care, valuable insight about the process can be obtained.

Extrusion process has been studied by means of different researchers in recent years because of its great importance in the industrial sector. Among different forming processes which are applicable for producing a bimetal rod, extrusion has some unique advantages over other processes such as rolling and drawing. The compressive state of stress and the possibility of producing metallurgical bonds between the two metals in extrusion makes this process a suitable choice for producing bimetal rods [1,2]. One of the most widely used bimetal materials is bimetal rods consisting of Al and Cu. In comparison with a Cu rod, the bimetallic rod is 40–60% lighter and 30–40% cheaper [1]. Some studies concerning the extrusion of bimetal rods have been presented. For example, Avitzur et al. [3] used the upper bound method to analyze fracture of the core, whilst Osakada et al. [4] used the energy method to discuss the occurrence of necking in the hard core layer. Tokuno and Ikeda [5] verified the deformation in extrusion of composite rods by experimental and upper bound methods. Yang et al. [6] studied the extrusion of composite rods through curved dies by experimental and upper bound methods. Sliwa [7] proposed a velocity field for the extrusion of composite rods, but his model is restricted to extrusion with a large angle of the die. Chitkara and Aleem studied the mechanics of extrusion of bimetallic tubes from solid circular billets using fixed mandrel with application of generalized upper bound analyses [8]. They investigated the effect of different parameters such as extrusion ratio, frictional conditions, and shape of the dies and that of the mandrels on the extrusion pressures. Kang et al. [10] designed the die for hot forward and backward extrusion process of Al/Cu clad composite by

♠Corresponding author, e-mail: hhaghighat@razi.ac.ir

experimental investigations and FEM simulations. Hwang [11] studied the plastic deformation behaviour within a conical die during composite rod extrusion by experimental and upper bound methods. They assumed the interface as a line segment. Kazanowski et al. [12] discussed the influence of initial bi-material billet geometry on the final product dimensions. The flat faced die used for all experiments and the proposed bimaterial billet design modifications evaluated experimentally and by finite element modelling using the Deform 3D system. Nowotynska and Smykla [13] studied the influence of die geometric parameters on plastic flow of layer composites during extrusion process by experimental method. Khosravifard and Ebrahimi [14] analyzed the extrusion of Al/Cu bimetal rods through conical dies by FEM and studied the effects of the extrusion parameters in creation of interfacial bonds. FEM needs more calculation resources and a good code knowledge by the users. Haghighat and Asgari [15] proposed a generalized spherical velocity field for bimetal tube extrusion process through dies of any shape. They assumed the boundaries at the entrance and the exit of the deformation zone as two concentric spherical surfaces with their centres at the intersection of the die surface with mandrel surface.

Most of mentioned analyses were based on fixed velocity fields, which cannot incorporate the effects of lubrication conditions, reduction in area and the die angle. These analyses for bimetal rod extrusion, however, were incapable of predicting the final thicknesses of the constituent materials with sufficient accuracy.

Experimental observations [5,6] and computational results by the finite element method [7] reveal that

1- The velocity field and the deformation region vary according to the die angle, reduction in area and lubrication conditions.

2-The interface surface between two metals in the deformation zone is a curve segment.

3-The particles in deformation zone move in the curved paths.

These facts show a particle, in deformation zone, has both radial and circumferential velocity components. In order to cover these drawbacks in upper bound analysis, in the present article, we begin in the next section with the derivation of the velocity field for mono-metal rod by assuming the boundary at the entrance into the deformation zone as an arbitrarily curved surface and the boundary at the exit as a spherical surface. Then, by minimizing the extrusion power formulated from the derived velocity field the optimized plastic boundary are determined. A further discussion and comparison with FEM simulation results for the extrusion of bimetal rods composed of copper and aluminum are presented.

2. MONO-METAL ROD EXTRUSION ANALYSIS

Fig. 1 shows a schema of the mono-metal rod extrusion process through a conical die. The billet considered for analysis is a rod with the initial and final radial of R_i and R_0, respectively.

2.1. Velocity Fields in Deformation Zones

The first step in modeling a metal forming operation by the upper bound method is to choose a velocity field for the material undergoing plastic deformation. As shown in Fig. 1, the material is divided into three zones in which the velocity field is continuous. In zones I and III the materials are rigid and move as rigid bodies with the velocity V_i in the extrusion direction; after extrusion, the rod moves with the velocity V_f in the axial direction.

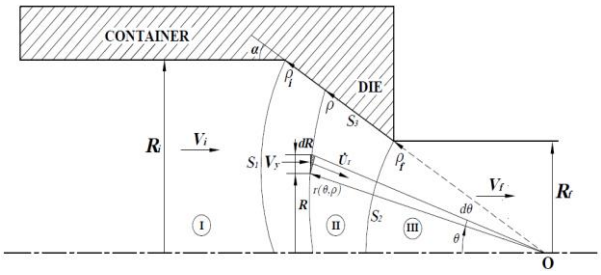

Fig. 1. Deformation zones for mono-metal rod extrusion process.

Zone II is the deformation region. From the volume flow balance, we have

$$V_i = \frac{R_f^2}{R_i^2} V_f \tag{1}$$

The shear boundary at the outlet of the deformation zone is assumed to be spherical surface with its center at the virtual apex of cone of the die and in the spherical coordinate system r, θ, φ is given by equation

$$r_f = \rho_f = \frac{R_f}{\sin\alpha} \tag{2}$$

Shear boundary of S_1 is assumed to be portion of exponential surface and it is represented mathematically by equation

$$r(\theta, \rho_i) = \rho_i \exp[\frac{b(\theta - \alpha)}{\alpha}] \tag{3}$$

Quantity b is geometric parameter of the shape of the boundary at the inlet of the deformation zone II. Quantity b can assume negative, zero or positive values. When b is negative, the inlet boundary moves away from the origin O, when b is positive the boundary move towards the apex of the die, when b is equal to zero, the inlet shear boundary is a spherical surface and in this case, (i.e. $g = 1$), Eq. (3) reduces to the shear surface proposed by Avitzur for flow through a conical die [7].

The function of the boundary for equal axial components of velocity in the deformation zone II may be expressed as

$$r(\theta,\rho)=\rho\exp[\frac{b(\theta-\alpha)}{\alpha}\frac{\rho-\rho_f}{\rho_i-\rho_f}]=\rho g(\theta,\rho) \quad (4)$$

where ρ is the radius at arbitrary equal axial components of velocity and

$$g(\theta,\rho)=\exp[\frac{b(\theta-\alpha)}{\alpha}\frac{\rho-\rho_f}{\rho_i-\rho_f}] \quad (5)$$

For simplicity $g(\theta,\rho)$ and $r(\theta,\rho)$ will be abbreviated to g and r, respectively. In zone II, because volume does not change, the component of the radial velocity becomes (see Fig. 1)

$$V_y\,2\pi R(dR)=-\dot{U}_r\,2\pi r\sin\theta(r\,d\theta) \quad (6)$$

and thus

$$\dot{U}_r=-\frac{V_y}{r}\frac{dR}{d\theta}=-V_i(\frac{\rho_i}{\rho})^2(\cos\theta+\frac{1}{g}\frac{\partial g}{\partial\theta}\sin\theta) \quad (7)$$

The full velocity field for the flow of the material in deformation zone II is obtained by invoking volume constancy. Volume constancy in spherical coordinate system is defined as

$$\dot{\varepsilon}_{rr}+\dot{\varepsilon}_{\theta\theta}+\dot{\varepsilon}_{\varphi\varphi}=0 \quad (8)$$

The strain rates in spherical coordinates are defined as

$$\dot{\varepsilon}_{rr}=\frac{\partial\dot{U}_r}{\partial r}$$

$$\dot{\varepsilon}_{\theta\theta}=\frac{1}{r}\frac{\partial\dot{U}_\theta}{\partial\theta}+\frac{\dot{U}_r}{r}$$

$$\dot{\varepsilon}_{\varphi\varphi}=\frac{1}{r\sin\theta}\frac{\partial\dot{U}_\varphi}{\partial\varphi}+\frac{\dot{U}_r}{r}+\frac{\dot{U}_\theta}{r}\cot\theta$$

$$\dot{\varepsilon}_{r\theta}=\frac{1}{2}(\frac{\partial\dot{U}_\theta}{\partial r}-\frac{\dot{U}_\theta}{r}+\frac{1}{r}\frac{\partial\dot{U}_r}{\partial\theta})$$

$$\dot{\varepsilon}_{\theta\varphi}=\frac{1}{2}(\frac{1}{r\sin\theta}\frac{\partial\dot{U}_\theta}{\partial\varphi}+\frac{1}{r}\frac{\partial\dot{U}_\varphi}{\partial\theta}-\frac{\cot\theta}{r}\dot{U}_\varphi)$$

$$\dot{\varepsilon}_{\varphi r}=\frac{1}{2}(\frac{\partial\dot{U}_\varphi}{\partial r}-\frac{\dot{U}_\varphi}{r}+\frac{1}{r\sin\theta}\frac{\partial\dot{U}_r}{\partial\varphi}) \quad (9)$$

For the rod extrusion, $\dot{U}_\varphi=0$ and a full velocity field is obtained by placing $\dot{U}_r$, from Eq. (6) into Eqs. (7)-(8), solving for $\dot{U}_\theta$ and applying boundary conditions for die axis and for the die surface we have

$$\dot{U}_\theta=V_i\frac{\rho_i^2}{\rho}\frac{\partial g}{\partial r}\sin\theta \quad (10)$$

Where

$$\frac{\partial g}{\partial r}=\frac{\partial g}{\partial\rho}\frac{\partial\rho}{\partial r}=\frac{b(\theta-\alpha)}{\alpha}\frac{1}{\rho_i-\rho_f}\frac{1}{1+\frac{b(\theta-\alpha)}{\alpha}\frac{\rho}{\rho_i-\rho_f}} \quad (11)$$

Therefore the velocity components in deformation zone II are given as

$$\dot{U}_r=-V_i(\frac{\rho_i}{\rho})^2(\cos\theta+\frac{1}{g}\frac{\partial g}{\partial\theta}\sin\theta)$$

$$\dot{U}_\theta=V_i\frac{\rho_i^2}{\rho}\frac{\partial g}{\partial r}\sin\theta$$

$$\dot{U}_\varphi=0 \quad (12)$$

Where

$$\frac{\partial g}{\partial r}=\frac{b(\theta-\alpha)}{\alpha}\frac{1}{\rho_i-\rho_f}\frac{1}{1+\frac{b(\theta-\alpha)}{\alpha}\frac{\rho}{\rho_i-\rho_f}} \quad (13)$$

Based on the established velocity field, the strain rates in the deformation zone can be given in usual matter. The six relationships to determine the strain rates components in deformation zone IIs are;

$$\dot{\varepsilon}_{rr} = -V_i \frac{\rho_i^2}{\rho^3}\frac{1}{g^2}[2(\rho\frac{\partial g}{\partial r}-1)g\cos\theta+(-2\frac{\partial g}{\partial\theta}+\rho\frac{\partial g}{\partial r}\frac{\partial g}{\partial\theta}+g\rho\frac{\partial^2 g}{\partial r\partial\theta})\sin\theta)]$$

$$\dot{\varepsilon}_{\theta\theta} = V_i(\frac{\rho_i}{\rho})^2\frac{1}{g}[(\frac{\partial^2 g}{\partial r\partial\theta}-\frac{1}{g}\frac{\partial g}{\partial\theta})\sin\theta+(\frac{\partial g}{\partial r}-\frac{1}{\rho})\cos\theta]$$

$$\dot{\varepsilon}_{\varphi\varphi} = V_i(\frac{\rho_i}{\rho})^2\frac{1}{g}[(-\frac{1}{\rho}+\frac{\partial g}{\partial r})\cos\theta+\frac{1}{g}\frac{\partial g}{\partial\theta}\sin\theta]$$

$$\dot{\varepsilon}_{r\theta} = \frac{1}{2}V_i(\frac{\rho_i}{\rho})^2\frac{1}{g}\{[-2\frac{\partial g}{\partial r}+\rho(\frac{\partial g}{\partial r})^2+\rho g\frac{\partial^2 g}{\partial r^2}+\frac{1}{\rho}[-1-\frac{1}{g^2}(\frac{\partial g}{\partial\theta})^2+\frac{1}{g}\frac{\partial^2 g}{\partial\theta^2}]]\sin\theta+\frac{1}{\rho}\frac{1}{g}\frac{\partial g}{\partial\theta}\cos\theta\}$$

(14)

2.3. Upper Bound Analysis

The total deforming power required for the process can be split up into three parts:

(a) Internal power of deformation;

(b) The power loss due to shear at surfaces of the velocity discontinuities; and

(c) The power loss due to friction along the die-material interface.

Thus, with reference to Fig. 1, the total power equals the sum of internal power of deformation for zone II, power loss at the velocity discontinuities S_1 and S_2 and the power loss due to friction on die surface S_3. The internal power of deformation can be calculated as follows

$$\dot{W}_i = \frac{2}{\sqrt{3}}\sigma_0\int_V\sqrt{\frac{1}{2}\dot{\varepsilon}_{ij}\dot{\varepsilon}_{ij}}\,dV \tag{15}$$

where σ_0 is the mean flow stress of the material and dV is a differential volume in the deformation zone.

$$dV = 2\pi\rho^2 g^2(g+\rho\frac{\partial g}{\partial\rho})\sin\theta\, d\theta\, d\rho \tag{16}$$

Thus, the equation to calculate the internal power of deformation in zone II is

$$\dot{W}_i = \frac{4\pi}{\sqrt{3}}\sigma_0\int_0^{\alpha}\int_{\rho_f}^{\rho_i}\sqrt{\frac{1}{2}\dot{\varepsilon}_{rr}^2+\frac{1}{2}\dot{\varepsilon}_{\theta\theta}^2+\frac{1}{2}\dot{\varepsilon}_{\varphi\varphi}^2+\dot{\varepsilon}_{r\theta}^2}\,\rho^2 g^2(g+\rho\frac{\partial g}{\partial\rho})\sin\theta\, d\theta\, d\rho \tag{17}$$

where σ_0 is the mean flow stress of the material. In upper bound method (which includes surfaces of velocity discontinuity), the integration of the shear strength of the material times the tangential velocity difference along the specified surface yields a finite quantity of power. This power loss is given by

$$\dot{W}_S = \frac{\sigma_0}{\sqrt{3}}\int_{S_v}|\Delta v|\,dS \tag{18}$$

The magnitude of the velocity discontinuity across surface S_1 can be written as

$$|\Delta v_1| = V_i\sqrt{1+(\frac{b}{\alpha})^2}(1-\rho_i\frac{\partial g}{\partial r})\sin\theta \tag{19}$$

An element of the surface area for S_1 is

$$dS_1 = 2\pi\rho_i^2 g^2(\theta,\rho_i)\sqrt{1+(\frac{b}{\alpha})^2}\sin\theta d\theta \tag{20}$$

Substituting equation (21) for dS, inserting the amount of the velocity discontinuity of equation (20) into equation (19) and simplifying, it follows

$$\dot{W}_{S_1} = \frac{2\pi}{\sqrt{3}}\sigma_0\rho_i^2 V_i[1+(\frac{b}{\alpha})^2]\int_0^{\alpha}(1-\rho_i\frac{\partial g}{\partial r})g^2(\theta,\rho_i)\sin\theta d\theta \tag{21}$$

For shear surface S_2, the amount of the velocity discontinuity is

$$|\Delta v_2| = V_f(1-\rho_f\frac{\partial g}{\partial r})\sin\theta,\qquad dS_2 = 2\pi(\rho_f\sin\theta)\rho_f\, d\theta \tag{22}$$

Thus the shear power consumed along shear boundary S_2

$$\dot{W}_{S_2} = \frac{2\pi}{\sqrt{3}}\sigma_0 V_f\rho_f^2\int_0^{\alpha}(1-\rho_f\frac{\partial g}{\partial r})\sin^2\theta\, d\theta \tag{23}$$

Assuming the friction stress to be a constant proportion of the flow stress of the material, it can be written

$$\dot{W}_f = m\frac{\sigma_0}{\sqrt{3}}\int_{S_f}|\Delta v|dS \qquad (24)$$

Where m is the constant friction factor. Frictional power is dissipated along the conical surface of the die, surface S_3 in Fig. 1, the magnitude of the velocity discontinuity becomes

$$|\Delta v_3| = V_i\left(\frac{\rho_i}{\rho}\right)^2\left(\cos\alpha + \frac{b}{\alpha}\frac{\rho-\rho_f}{\rho_i-\rho_f}\sin\alpha\right), \quad dS_3 = 2\pi\rho\sin\alpha\, d\rho \qquad (25)$$

Thus

$$\dot{W}_f = \frac{2\pi}{\sqrt{3}}m\sigma_0 V_i\rho_i^2\sin\alpha\int_{\rho_f}^{\rho_i}\frac{1}{\rho}\left(\cos\alpha + \frac{b}{\alpha}\frac{\rho-\rho_f}{\rho_i-\rho_f}\sin\alpha\right)d\rho \qquad (26)$$

The effect of friction in the container is neglected in this study. Therefore, the frictional power loss along the container surface is vanished. The externally supplied power is given by

$$\dot{W}_{ext} = F_e V_i = \dot{W}_i + \dot{W}_{S_1} + \dot{W}_f + \dot{W}_{S_2} \qquad (27)$$

where F_e is the required extrusion force. In accordance with the usual practice of the upper bound method, the external power $\dot{W}_{ext}$ can be equated to the sum of all the powers consumed. Therefore, the total upper bound solution for extrusion force is given by

$$F_e = \frac{\dot{W}_i + \dot{W}_{S1} + \dot{W}_{S2} + \dot{W}_f}{V_i} \qquad (28)$$

Consideration equation (31) reveals that the extrusion force required for rod extrusion becomes a function of the process parameters (radii of initial billet and final rod, friction factor and semi die angle) and the parameter associated with the velocity field, quantity b which determine the shape of the inlet boundary of deformation zone. Therefore, minimization of equation (31) with respect to b will yield a lower upper bound solution for the extrusion force. Thus, the lowest upper bound value of the relative extrusion force is obtained among its family of boundary shapes. A computer program was used to perform the minimization process.

3. BIMETAL ROD EXTRUSION PROCESS ANALYSIS

Fig. 2 shows a schema of the extrusion process of an initially bonded bimetal rod through a conical die. The billet considered for analysis is a bimetal rod made up of a rod and an annular tube of two different ductile materials with the mean flow stresses, σ_{0c} and σ_{0s}. The subscripts c and s denote core and sleeve, respectively. The initial outer and the interface of the initial billet radii of are R_i and R_{ic}, respectively. The outer radius of the extruded bimetal rod is R_{1f} and the interface radius of the final extruded rod is R_{2f}.

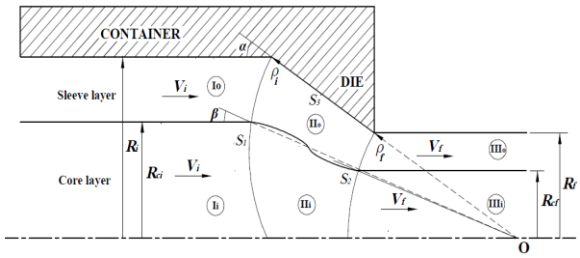

Fig. 2. Deformation zones for bonded bimetal rod extrusion process.

It is assumed that before and after the commencement of the extrusion, bond exists between two metals. Hence, there is not a relative motion between the metals whilst they are deforming. It then follows from material continuity that the materials must deform at different rates and therefore each material suffers a different strain.

3.1. Velocity Fields in Deformation Zones

The kinematically admissible velocity field which explained in Section 2, is applied to the case of extrusion of a bimetal rod as shown in Fig. 2. Each layer of the bimetal rod is divided into three zones in which the velocity field is continuous. In zones Is, Ic, IIIs and IIIc the materials are rigid and move as rigid bodies. Before entering the die, each constituent material of the bimetal rod moves as a rigid body with the same velocity V_i in the extrusion direction; after extrusion, the bimetal rod moves with the velocity V_f in the axial direction. It then follows that each metal deforms to a different reduction. Zones IIs and IIc are the deformation regions. The shear boundary at the outlet of the deformation zone S_2, is assumed to be spherical surface with its centers at the virtual apex of cone of the die and in the spherical coordinate system (r,θ,φ) is given by equation

$$\rho_f = \frac{R_f}{\sin\alpha} = \frac{R_{2f}}{\sin\beta_2} \qquad (29)$$

In deformation zone IIs, the velocity field can be given by Eq. (12).

The angle β_1 of the interface at the inlet shear boundary, shown in Fig. 2, is given by solving the following equation

$$\tan\beta_1 = \frac{R_{ci}}{\rho_i \exp[\frac{b(\beta_1-\alpha)}{\alpha}]} \quad (30)$$

From continuity of material, the angle β_2, shown in Fig. 2, is given by

$$\sin\beta_2 = \frac{R_{ci}}{R_i}\sin\alpha \quad (31)$$

3.2.1. Calculation of the power terms

Referring to Fig. 2, the total power equals the sum of internal power of deformation for zones IIs and IIc, power loss at the velocity discontinuity surfaces S_1 and S_2 and the power loss due to friction on die surface S_3 .The equation to calculate the internal power of deformation in zone IIs is

$$\dot{W}_{is} = \frac{4\pi}{\sqrt{3}}\sigma_{0s}\int_{\beta(\rho)}^{\alpha}\int_{\rho_f}^{\rho_i}\sqrt{\frac{1}{2}\dot{\varepsilon}_{rr}^2+\frac{1}{2}\dot{\varepsilon}_{\theta\theta}^2+\frac{1}{2}\dot{\varepsilon}_{\varphi\varphi}^2+\dot{\varepsilon}_{r\theta}^2}\,\rho^2 g^2(g+\rho\frac{\partial g}{\partial\rho})\sin\theta\, d\theta\, d\rho \quad (32)$$

where $\beta(\rho)$ is the angular position of the each point on the interface and σ_{0s} is the mean flow stress of the sleeve material and is given by

$$\sigma_{os} = \frac{\int_0^{\varepsilon}\sigma_s\, d\varepsilon}{\varepsilon}, \quad \varepsilon = \ln\frac{{R_i}^2-{R_{ci}}^2}{{R_f}^2-{R_{cf}}^2} \quad (33)$$

The equation to calculate the internal power of deformation in zone IIc is

$$\dot{W}_{ic} = \frac{4\pi}{\sqrt{3}}\sigma_{0c}\int_{0}^{\beta(\rho)}\int_{\rho_f}^{\rho_i}\sqrt{\frac{1}{2}\dot{\varepsilon}_{rr}^2+\frac{1}{2}\dot{\varepsilon}_{\theta\theta}^2+\frac{1}{2}\dot{\varepsilon}_{\varphi\varphi}^2+\dot{\varepsilon}_{r\theta}^2}\,\rho^2 g^2(g+\rho\frac{\partial g}{\partial\rho})\sin\theta\, d\theta\, d\rho \quad (34)$$

where σ_{0c} is the mean flow stress of the core material and is given by

$$\sigma_{oc} = \frac{\int_0^{\varepsilon}\sigma_c\, d\varepsilon}{\varepsilon}, \quad \varepsilon = \ln\frac{{R_{ci}}^2}{{R_{cf}}^2} \quad (35)$$

The shear power consumed along shear boundary S_1 can be split up into two parts and

$$\dot{W}_{S_{1c}} = \frac{2\pi}{\sqrt{3}}\sigma_{0c}\rho_i^2 V_i[1+(\frac{b}{\alpha})^2]\int_0^{\beta_1}(1-\rho_i\frac{\partial g}{\partial r})g^2(\theta,\rho_i)\sin\theta d\theta \quad (36)$$

$$\dot{W}_{S_{1s}} = \frac{2\pi}{\sqrt{3}}\sigma_{0s}\rho_i^2 V_i[1+(\frac{b}{\alpha})^2]\int_{\beta_1}^{\alpha}(1-\rho_i\frac{\partial g}{\partial r})g^2(\theta,\rho_i)\sin\theta d\theta \quad (37)$$

The shear power consumed along shear boundary S_2 is

$$\dot{W}_{S_{2c}} = \frac{2\pi}{\sqrt{3}}\sigma_{0c}V_f\rho_f^2\int_0^{\beta_2}(1-\rho_f\frac{\partial g}{\partial r})\sin^2\theta d\theta \quad (38)$$

$$\dot{W}_{S_{2s}} = \frac{2\pi}{\sqrt{3}}\sigma_{0s}V_f\rho_f^2\int_{\beta_2}^{\alpha}(1-\rho_f\frac{\partial g}{\partial r})\sin^2\theta d\theta \quad (39)$$

The frictional power losses along the die surface is calculated by Eq. (29) by placing σ_{0s} instead of σ_0 .

Therefore, the total upper bound solution for extrusion force is given by

$$F_e = \frac{\dot{W}_{is} + \dot{W}_{ic} + \dot{W}_{S1s} + \dot{W}_{S2s} + \dot{W}_{S1c} + \dot{W}_{S2c} + \dot{W}_f}{V_i} \quad (40)$$

As mentioned earlier, each constituent layer may not deform homogeneously owing to dissimilar mechanical properties. Thus, the exit radius ratio of the core/sleeve differs from those of the assembled billet. Herein, parameter b is introduced to account for this non-homogeneous deformation. Therefore, minimization of above equation with respect to b will yield a lower upper bound solution for the extrusion force and predict the final thickness of each material.

4. RESULTS AND DISCUSSION

To make a comparison with the developed analytical model, initially bonded bimetal rods composed of aluminium as core and copper as sleeve, were used. The configuration of the sleeve and core layers is shown in Fig. 3.

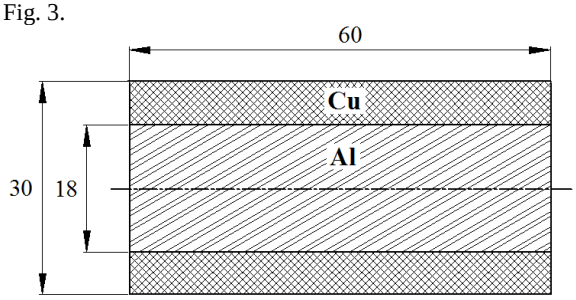

Fig. 3. Configuration of the bimetal rod before extrusion (dimensions are in mm).

The flow stresses for copper and aluminium in room temperature obtained as [11]

$$\sigma_{Al} = 189.2\ \varepsilon^{0.239}\ \text{MPa} \quad (41)$$

$$\sigma_{Cu} = 335.2\ \varepsilon^{0.113}\ \text{MPa} \quad (42)$$

The relative extrusion pressure as a function of b for α =10° and α =30° and RA=25 are plotted in Fig. 4. The value of b at which the relative extrusion pressure is minimum. In the present research, FEM analysis is performed by ABAQUS software package.

Considering the symmetry in geometry, two dimensional axi-symmetric models are used for FEM analyses. The die is assumed as a rigid model. Since the analytical rigid option is used for the rigid bodies, they are not meshed.The bimetal rod has been meshed with the CGAX4R element. This type of elements belongs to the ABAQUS element library. The die model is fixed in other directions by applying displacement constraint on its nodes while the punch model is loaded by specifying displacement in the axial direction. The most common means of comparing upper bound and FEM results is through extrusion force. Values for the extrusion forces

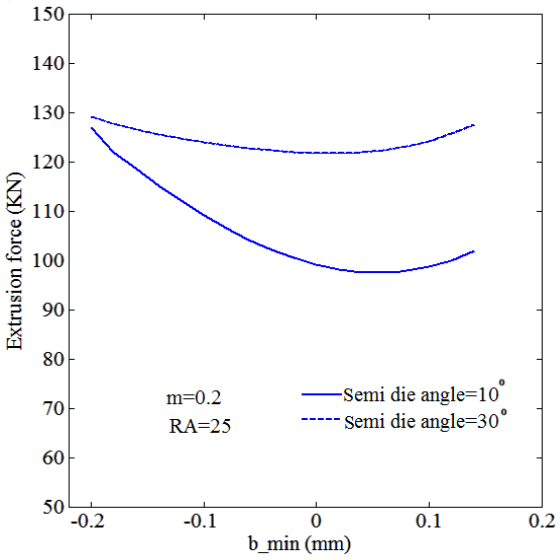

Fig. 4. Variation of extrusion force with b for α =10° and α =30°.

are evaluated from the FEM results.

Fig. 5a illustrates the mesh used to analyze the deformation in extrusion of bi-metallic rod for conical die shape and the extrusion conditions R_i = 15mm, R_{ic} = 9mm, reduction in area 15% and the m = 0.2. Fig. 5b shows uniform deformation.

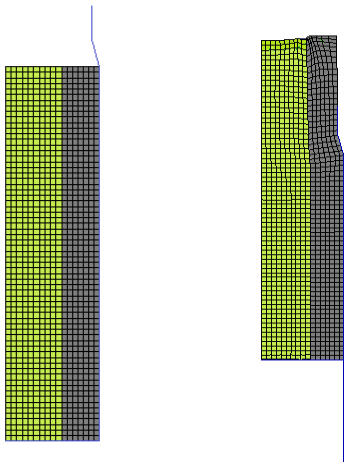

(a) (b)

Fig. 5. (a) The finite element mesh, (b) The deformed mesh (R_i = 15 mm, R_{ic} = 9 mm, reduction in area = 15%).

In Fig. 6, the extrusion forces obtained from the upper bound solution are compared with the experimental results obtained from Ref. [11] for conical die with $\alpha = 15°$. The extrusion conditions are R_i = 15mm, R_{ic} = 9mm, $m = 0.2$ and three different reductions in

areas, RA=25, 50 and 66.7% are adopted during the analytical solution and the FEM simulation.
The results show good agreement between the analysis and experiment. In that figure, it is possible to see that analytical solutions are bigger than FEM ones. Obviously, the extrusion force increases with increasing area reduction.

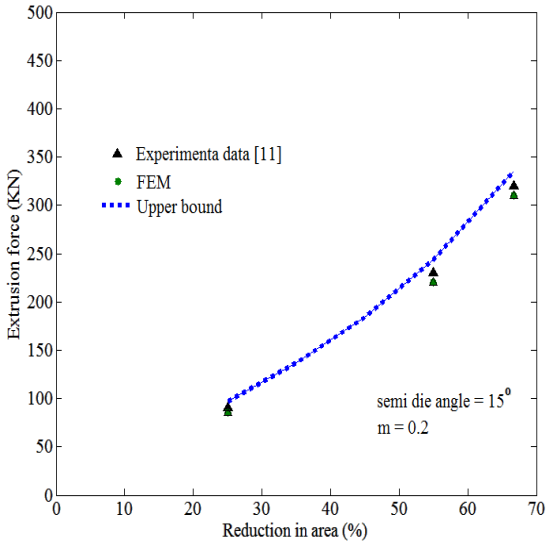

Fig. 6. Comparison of analytical, FEM and experimental of [11] for $\alpha = 15^{\circ}$.

Die angle has a great influence on the deformation mode as well as on extrusion force as shown in Fig. 7. Figure 7 shows the optimal die geometry and plastic boundaries for different friction factors at two reductions of area (RA = 40 and 60). For the given reduction in area the optimal die angle becomes greater with increasing friction factor and the deformation zone flushes upstream.

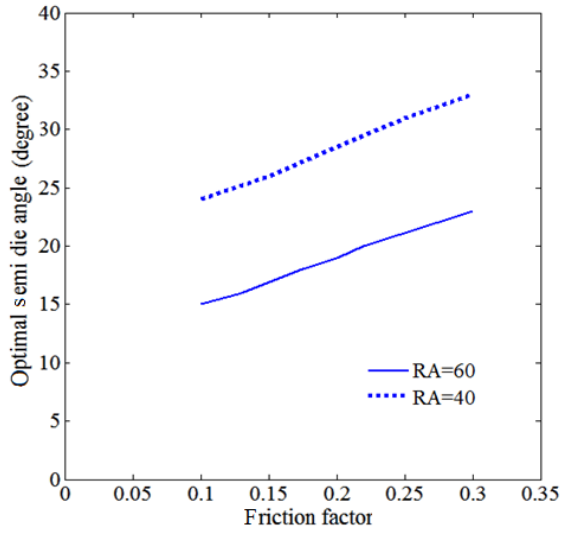

Fig. 7. Variation of optimal die geometry with m for RA = 40 and 60.

The theoretically predicted values of the final thickness of each layer can also be assessed, considering the variation of area reduction of core and sleeve with that of the composite. For example, in Fig. 8, the area reductions of the aluminum core and copper sleeve are plotted against the total reduction for the semi die angle of 25°. This figure also reveals the close agreement existing between the two sets of results.

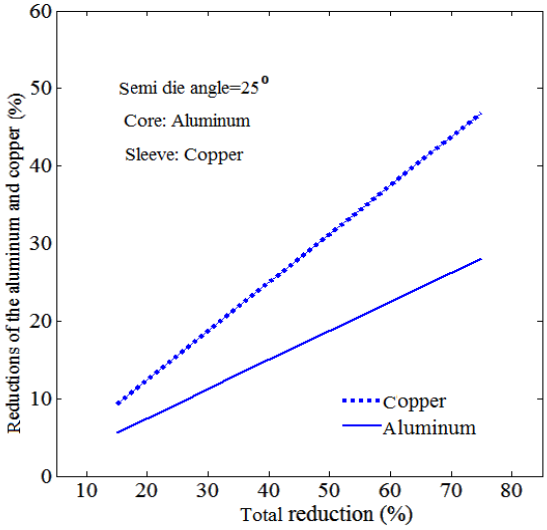

Fig. 8. Variation the area reductions of the aluminum core and copper sleeve against the total reduction.

The effect of semi-angle of die upon extrusion force in reduction in area 25% and 50% is shown in Fig. 9. The results show that for each reduction in area, there is an optimum angle, and optimum semi-angle of die increases with increasing reduction in area, see Fig. 9. It is observed that, for each case there is an optimal die angle, which minimizes the extrusion force. It is seen that the optimal die angle becomes shorter with decreasing reduction in area.

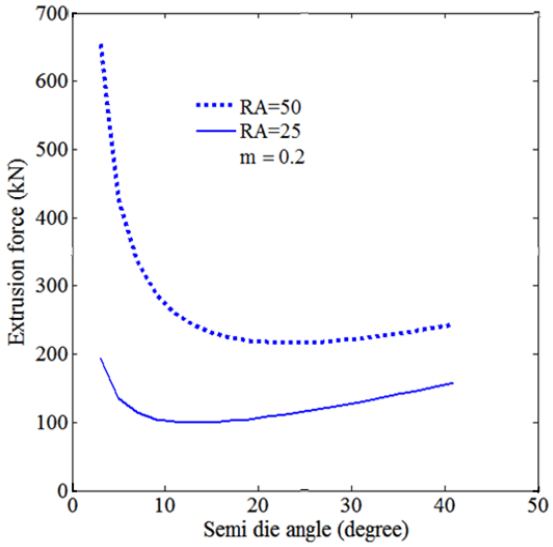

Fig. 9. Effect of semi-angle of die upon the extrusion force.

The effect of die angle on the extrusion force for different values of friction factor is shown in Fig. 10. As it is expected, for a given value of friction factor, there is an optimum die angle in which the extrusion force is minimized. It is also observed that the optimum die angle increasing when shearing friction factor increases. From this figure, it is also seen that an increase in the friction factor tends to increase the extrusion force.

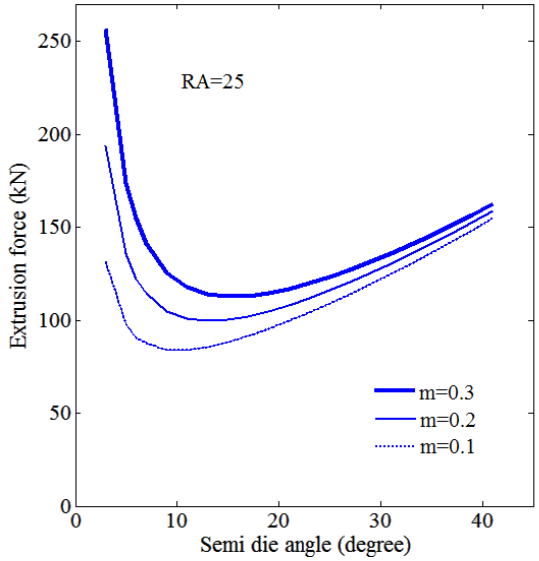

Fig. 10. The effect of die angle on the extrusion force for different values of friction factor.

5. CONCLUSIONS

This paper presented a generalized expression for the flow field generated by the plastic flow of metal in extrusion process through a conical die. It has advantageous for finding a better upper bound value of the extrusion force and corresponding optimal die angle. The analytical results by the present method show a good coincidence with the results by the finite element method.

1-According to this subject that, the value of b at which the relative extrusion pressure is a minimum, represents the assumed inlet boundary of the plastic zone during actual flow.
2- It can be inferred the optimal die angle becomes greater with increasing friction factor and the deformation zone flushes upstream.
3- The results show that for each reduction in area, there is an optimum die angle, and optimum semi-angle of die increases with increasing reduction in area.
4-The optimum die angle decreases when shearing friction factor increases and increase in the friction factor tends to increase the extrusion force.

CONFLICT OF INTEREST

No conflict of interest was declared by the authors.

REFERENCES

[1] Ahmed N. Extrusion of copper clad aluminum wire. J Mech Work Technol 1978;2:19–32.

[2] Berski S, Dyja H, Banaszek G, Janik M. Theoretical analysis of bimetallic rod extrusion process in double reduction die. J Mater Process Technol 2004;153–154:583–8.

[3] B. Avitzur, R.Wu, S. Talbert, Y.T.Chou, Criterion for the Prevention of Core Fracture During Extrusion of Bimetal Rods, Journal of Engineering for Industry, 1982, Vol. 104, pp. 293-304.

[4] Osakada, K, Limb, M & Mellor, PB 1973, Hydrostatic extrusion of composite rods with hard cores, International Journal of Mechanical Sciences, vol. 15, pp. 291-307.

[5] Tokuno, H & Ikeda, K 1991, Analysis of deformation in extrusion of composite rods, Journal of Materials Processing Technology, vol. 26, pp. 323-335.

[6] Yang, DY, Kim, YG & Lee, CM 1991, An upper-bound solution for axisymetric extrusion of composite rods through curved dies, International Journal of Mechanical Sciences, vol. 31, pp. 565-575.

[7] Sliwa, R 1997, Plastic zones in the extrusion of metal composites, Journal of Materials Processing Technology, vol. 67, pp. 29-35.

[8] Chitkara, NR & Aleem, A 2001a, Extrusion of axi-symmetric bi-metallic tubes from solid circular billets: application of a generalized upper bound analysis and some experiments, International Journal of Mechanical Sciences, vol. 43, pp. 2833-2856.

[9] Chitkara, NR & Aleem, A 2001b, Extrusion of axi-symmetric bi-metallic tubes: some experiments using hollow billets and the application of a generalized slab method of analysis, International Journal of Mechanical Sciences, vol. 43, pp. 2857–2882.

[10] Kang, CG, Jung, YJ & Kwon, HC 2002, Finite element simulation of die design for hot extrusion process of Al/Cu clad composite and its experimental investigation, Journal of Materials Processing Technology, vol. 124, pp. 49-56.

[11] Hwang, YM & Hwang, TF 2002, An investigation into the plastic deformation behavior within a conical die during composite rod extrusion, Journal of Materials Processing Technology, vol. 121, pp. 226-233.

[12] Kazanowski, P, Epler, ME & Misiolek, WZ 2004, Bi-metal rod extrusion-process and product optimization, Materials Science and Engineering A, vol.369, pp. 170–180.

[13] Nowotynska, I & Smykla, A 2009, Influence of die geometric parameters on plastic flow of Layer composites during extrusion process, Journal of Materials Processing Technology, vol. 209, pp. 1943-1949.

[14] Khosravifard, A., Ebrahimi, R., Investigation of parameters affecting interface strength in Al/Cu clad bimetal rod extrusion process, Materials and Design vol. 31, pp. 493-499, (2010).

[15] Haghighat, H, Asgari, GR 2011, A generalized spherical velocity field for bi-metallic tube extrusion through dies of any shape, International Journal of Mechanical Sciences, vol. 53, pp. 248-253.